Mathematics and Computers in Simulation 225 (2024) 513–527

Contents lists available at ScienceDirect

Mathematics and Computers in Simulation

journal homepage: www.elsevier.com/locate/matcom

Original articles

ENO and WENO cubic quasi-interpolating splines in Bernstein–Bézier form

F. Aràndiga [a,*], D. Barrera [b], S. Eddargani [c]

[a] Departament de Matemàtiques. Universitat de València (EG), Spain
[b] Department of Applied Mathematics, University of Granada, Campus de Fuentenueva s/n, 18071 Granada, Spain
[c] Department of Mathematics, University of Rome Tor Vergata, 00133 Rome, Italy

ARTICLE INFO

Keywords:
Bernstein–Bézier representation
Quasi-interpolation
WENO-ENO

ABSTRACT

In this paper we propose the use of C^1-continuous cubic quasi-interpolation schemes expressed in Bernstein–Bézier form to approximate functions with jumps. The construction of these schemes is explicit and consists of directly attaching the Bernstein–Bézier coefficients to appropriate combinations of the given data values. This construction can lead to quasi-interpolation schemes with free parameters. This allows to write these schemes of optimal convergence order as a non-negative convex combination of certain quasi-interpolation schemes of lower convergence order. The idea behind that, is to divide the data set used to define a quasi-interpolant of optimal order into subsets, and then define the associated quasi-interpolants. The free parameters facilitate the choice of the convex combination weights. We then apply the WENO approach to the weights to eliminate the Gibbs phenomenon that occurs when we approximate in a non-smooth region. The proposed schemes are of optimal order in the smooth regions and near optimal order is achieved in the neighboring region of discontinuity.

1. Introduction

Splines are piecewise functions glued together with certain smoothness conditions. They represent a fundamental tool in various applications, among them numerical solution of equations or systems of equations of differential, integral or integro-differential equations and their applications. Some of these applications imply the use of approximation methods to generate a spline function from discrete data. Interpolation and least squares are frequently used as popular methods. Both require the solution of a system of linear equations which have as equal number of unknowns as the dimension of the spline space, and then they are not convenient for real-time processing of large data streams. Furthermore, interpolation approach has to match the data at selected points and this requirement might be a problem in case of dealing with noisy data. To this end, local methods, that determine the spline coefficients using only local information, are more suitable. Besides, the methods should reproduce polynomials and preferably functions in the given spline space to ensure the best approximation properties. An example of a local method is the spline quasi-interpolation approach.

The quasi-interpolation approach is a powerful approximation method that was introduced by Schoenberg [24,25] for the approximation of functions and referred to as *smoothing interpolation*. It has several advantages, among them: quasi-interpolation is efficient and relatively easy to formulate for scattered and meshed nodes and for any number of data, and it is not necessary to solve any linear system of equations.

* Corresponding author.
E-mail addresses: arandiga@uv.es (F. Aràndiga), dbarrera@ugr.es (D. Barrera), eddargani@mat.uniroma2.it (S. Eddargani).

https://doi.org/10.1016/j.matcom.2024.06.001
Received 14 November 2023; Received in revised form 27 March 2024; Accepted 3 June 2024
Available online 5 June 2024

A linear quasi-interpolation operator Q maps a function f to an element

$$Qf = \sum_{i\in A} \lambda_i(f) N_i$$

of a suitable spline space S, where A, $\{\lambda_i(f),\, i \in A\}$ and $\{N_i,\, i \in A\}$, respectively are a set of indices linked to the information on the function to be approximated, a set of linear functionals and a set of spline functions spanning S. The reader can find more details on the spline quasi-interpolation construction in [1,8,10,11] and references therein.

The spline functions N_i should be locally supported and form a non-negative partition of unity. These properties are very important because they make the spline curve can be locally adapted in an intuitive and flexible way. Classical examples of a such basis are the Bernstein basis and any polynomial B-spline bases [9].

The functionals λ_i can be of different types, chosen according to the provided information about the function f to be approximated. Usually they are point [16,23], derivative [13] or integral linear functionals [15,22]. In this work, we consider the first case, in which $\lambda_i(f)$ is a finite linear combination of values of f.

The quasi-interpolation operator Q is defined to offer optimal convergence for smooth functions by imposing its exactness on the space of polynomials of maximal degree included in S, but in the presence of sharp jumps or discontinuities, it may result in overshooting and undershooting, known as Gibbs phenomenon [12]. Similar to Fourier series, this can lead to oscillations around jump discontinuities, reducing accuracy, particularly in non-smooth regions like image processing or shock capture schemes.

Coefficients $\lambda_i(f)$ are defined from discrete values of f within a stencil around the B-spline N_i. Discontinuities across this stencil lead to poor accuracy and over- or undershooting. Maximizing accuracy involves selecting stencils that avoid singularities, as done in the Essentially Non-Oscillatory (ENO) approach, introduced in [18]. ENO methods construct polynomials using information only smooth regions, and choosing stencils with the lowest smoothness indicator.

For greater flexibility, the Weighted-ENO (WENO) concept combines multiple stencils, improving accuracy [3,19]. WENO methods assign weights based on smoothness indicators and accuracy properties, enhancing performance in smooth regions and around discontinuities [17].

Choosing appropriate weights is crucial. They should form a convex combination favoring smooth stencils and minimizing contributions from those crossing singularities. Negative weights, a potential issue, are addressed in the literature, with techniques discussed in [4,26], ensuring non-negativity and preserving accuracy.

This paper explores approximating discrete values coming from functions with jump discontinuities using quasi-interpolating cubic splines in the Bernstein basis. Specifically, we focus on constructing C^1 cubic quasi-interpolation spline schemes in Bernstein–Bézier (BB-) form. These schemes are directly determined by fixing their BB-coefficients to suitable combinations of given data values, as initially introduced in the bivariate case in [5,7,27], with subsequent comprehensive studies in the univariate case in [6].

These constructions result in spline quasi-interpolation schemes with free parameters, offering flexibility to achieve additional properties such as super-convergence at specific points. In our approach, this flexibility is utilized in selecting non-negative weights for the WENO method. Unlike previous strategies, our method allows for non-unique weights, enabling users to tailor weights for each stencil by imposing conditions on the free parameters. This approach yields spline schemes of optimal order in smooth regions while mitigating Gibbs phenomena near singularity points.

The rest of paper is organized as follows. In Section 2 we define the cubic spline quasi-interpolation schemes in BB-form and see how it can be constructed. In Sections 3–5 we use nonlinear techniques (ENO and WENO) to obtain the BB-coefficients and we see the properties that each of the operators we obtain have. In Section 6, through numerical results, we validate the results obtained in the previous sections. Finally, in Section 7, we present some conclusions.

2. C^1 cubic spline quasi-interpolation schemes in BB-form

Let $P_n := \{a = x_0 < x_1 < \cdots < x_{n-1} < x_n = b\}$ be a partition of a bounded interval $I := [a, b]$ with equispaced knots $x_i := a + ih$, $i = 0, \ldots, n$, where $h := \frac{b-a}{n}$. It induces a decomposition of I into the subintervals $I_i := [x_i, x_{i+1}]$, $i = 0, \ldots, n-1$.

The space $S_3^1(P_n)$ of C^1 cubic polynomial splines on P_n is defined by

$$S_3^1(P_n) := \left\{ s \in C^1(I) : s_{|I_i} \in \mathbb{P}_3,\, i = 0, \ldots, n-1 \right\},$$

where $\mathbb{P}_3$ represents the linear space of cubic polynomials. The restriction of a spline $s \in S_3^1(P_n)$ to I_i, s_i, is a cubic polynomial, then it can be represented in terms of cubic Bernstein polynomials $\mathfrak{B}_\alpha(t) := \frac{3!}{\alpha_1!\,\alpha_2!}(1-t)^{\alpha_1} t^{\alpha_2}$, for an multi-index $\alpha := (\alpha_1, \alpha_2)$ with non-negative integer entries, relative to the unit interval $[0, 1]$. In general, the 1-norm of $\xi := (\xi_1, \ldots, \xi_d) \in \mathbb{R}^d$ is defined as $\|\xi\|_1 := |\xi_1| + \cdots + |\xi_d|$, so that the length of a multi-index α is equal to $\|\alpha\|_1 = \alpha_1 + \alpha_2$. The Bernstein polynomials $\mathfrak{B}_\alpha$, $\|\alpha\|_1 := 3$, form a basis of $\mathbb{P}_3$, and

$$s_i(x) = \sum_{\|\alpha\|_1 = 3} b_{\alpha,i} \mathfrak{B}_\alpha^i(x), \tag{1}$$

where $\mathfrak{B}_\alpha^i(x) := \mathfrak{B}_\alpha\left(\frac{x - x_i}{h}\right)$.

The restriction s_i is a linear combination of the BB-coefficients $b_{\alpha,i}$ with non-negative weights $\mathfrak{B}_\alpha^i$, so that the graph of s_i lies in the convex hull of the Bézier control points $\{(\xi_{\alpha,i}, b_{\alpha,i}), \|\alpha\|_1 = 3\}$, where each domain point $\xi_{\alpha,i} := \frac{\alpha_1}{3} x_i + \frac{\alpha_2}{3} x_{i+1}$ is naturally associated with the BB-coefficient $b_{\alpha,i}$. The Bézier control net represents the linear piecewise interpolant of the Bézier control points.

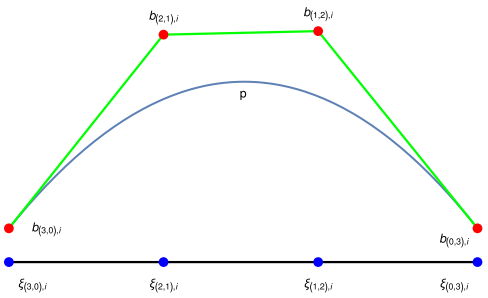

Fig. 1. Schematic representation of the BB-form of the cubic polynomial on I_i.

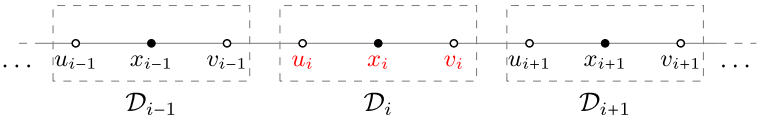

Fig. 2. Labeling the domain points of various sub-intervals.

Fig. 1 shows an example of a schematic representation of the domain points, Bézier control points, Bézier control net, and a spline curve that lies inside the convex hull of Bézier control points. The representation given in (1) is said to be the BB-form of s_i. It will be extensively used in this work to define the quasi-interpolating spline schemes.

Let $\mathcal{D} := \left\{a + i\frac{h}{3}, i = 0, \dots, 3n\right\}$ be the union without repetitions of the domain points associated with all the subintervals I_i, $i = 0, \dots, n-1$, and suppose that the discrete values $f\left(x_i\right)$ of a real function f at the knots of P_n are known. We are interested in the construction of quasi-interpolating spline schemes Qf in the space $S_3^1\left(P_n\right)$. The construction is explicit and consists in setting the BB-coefficients related to the domain points in $\mathcal{D}$. They will be linear combinations of a fixed number of point values of f.

We deal with the construction of a cubic quasi-interpolating Qf to f in the space $S_3^1\left(P_n\right)$ by setting directly the BB-coefficients of its restriction to each subinterval I_i. They will be linear combinations of a fixed number of point values of f. The partition is uniform, therefore, it is reasonable to think that it is possible to define the BB-coefficients in each of the intervals by defining a reduced number of them linked to well-selected domain points. For this purpose, we consider a specific partition of the set $\mathcal{D}$, namely, $\mathcal{D} = \bigcup_{0\le i\le n} \mathcal{D}_i$, with $\mathcal{D}_i := \left\{u_i, x_i, v_i\right\}$, where $u_i := x_i - \frac{h}{3}$ and $v_i := x_i + \frac{h}{3}$. In Fig. 2 the above partition is illustrated.

Following this notation, the restriction of the quasi-interpolant Qf on the sub-interval I_i can be rewritten as

$$Qf_{|_{I_i}}(x) = c\left(x_i\right)\mathfrak{B}^i_{(3,0)}(x) + c\left(v_i\right)\mathfrak{B}^i_{(2,1)}(x) + c\left(u_{i+1}\right)\mathfrak{B}^i_{(1,2)}(x) + c\left(x_{i+1}\right)\mathfrak{B}^i_{(0,3)}(x), \tag{2}$$

where $c(p)$ represents the BB-coefficient related to the domain point p. In Fig. 2 we can see the four domain points whose associated BB-coefficients are used in (2).

We will define the BB-coefficients of $Qf_{|_{I_i}}$ as linear combinations of the values of f at the neighboring knots.

Problem 1. Define for each knot x_i the stencil $S_i := \left\{x_{i-2}, x_{i-1}, x_i, x_{i+1}, x_{i+2}\right\}$, $i = 0, \dots, n$, and $f(S_i) := \left\{f\left(x_{i-2}\right), f\left(x_{i-1}\right), f\left(x_i\right), f\left(x_{i+1}\right), f\left(x_{i+2}\right)\right\}$. Find masks $\beta := \left(\beta_0, \beta_1, \beta_2, \beta_3, \beta_4\right)$, $\gamma := \left(\gamma_0, \gamma_1, \gamma_2, \gamma_3, \gamma_4\right)$ and $\delta := \left(\delta_0, \delta_1, \delta_2, \delta_3, \delta_4\right)$ such that the quasi-interpolant Qf defined in each interval I_i with BB-coefficients

$$c\left(u_i\right) :=< \delta, f(S_i) >, \quad c\left(x_i\right) :=< \beta, f(S_i) >, \quad c\left(v_i\right) :=< \gamma, f(S_i) >, \tag{3}$$

is C^1-continuous and $Qf = f$ is satisfied for all $f \in \mathbb{P}_3$.

For $p = \left(p_0, p_1, p_2, p_3, p_4\right)$ and $q = \left(q_0, q_1, q_2, q_3, q_4\right)$, the notation $< p, q >$ has been used to represent the value $\sum_{l=0}^4 p_l q_l$. The masks β, γ and δ have been asked to be interval-independent since the partition is uniform.

In view of the chosen stencils, working with functions defined on a bounded interval requires to properly define the BB-coefficients of the subintervals I_0, I_1, I_{n-1} and I_n. To facilitate the development of the ideas considered in this work, until otherwise stated, the functions and their quasi-interpolants will be defined on the real line, with the uniform partition $a + h\mathbb{Z}$.

Proposition 1. *The quasi-interpolant Qf defined by (2) and (3) is C^1-continuous if, and only if,*

$$2\beta_k = \gamma_k + \delta_k, \quad k = 0, \dots, 4.$$

Proof. We have that Qf is C^1-continuous if, and only if, $2c\left(x_i\right) - c\left(u_i\right) - c\left(v_i\right) = 0$ for all $i \in \mathbb{Z}$. Substituting the BB-coefficients $c\left(x_i\right)$, $c\left(u_i\right)$ and $c\left(v_i\right)$ by their expressions given in (3), it results

$$2c\left(x_i\right) - c\left(u_i\right) - c\left(v_i\right) = \Lambda_0 f\left(x_{i-2}\right) + \Lambda_1 f\left(x_{i-1}\right) + \Lambda_2 f\left(x_i\right) + \Lambda_3 f\left(x_{i+1}\right) + \Lambda_4 f\left(x_{i+2}\right), \tag{4}$$

where $\Lambda_k := 2\beta_k - \gamma_k - \delta_k$, $k = 0, \dots, 4$, from which the claim follows. □

Once the C^1-conditions have been imposed and characterized in terms of the masks, we must now establish the conditions that ensure the exactness on the space of cubic polynomials.

Lemma 2. *The BB-coefficients of the monomials* $m_k = \left(\frac{x-x_i}{h}\right)^k$, $k = 0, \dots, 3$, *restricted to the subinterval* I_i *are* $(1,1,1,1)$, $\left(0, \frac{1}{3}, \frac{2}{3}, 1\right)$, $\left(0, 0, \frac{1}{3}, 1\right)$ *and* $(0,0,0,1)$, *respectively.*

Now, we are in a position to solve Problem 1.

Proposition 3. *Problem 1 has infinitely many solutions, provided by the masks*

$$\beta = \{\lambda, -4\lambda, 6\lambda + 1, -4\lambda, \lambda\},$$
$$\gamma = \left\{\mu, -4\mu - \frac{1}{9}, 6\mu + \frac{5}{6}, \frac{1}{3} - 4\mu, \mu - \frac{1}{18}\right\},$$
$$\delta = \left\{2\lambda - \mu, -8\lambda + 4\mu + \frac{1}{9}, 12\lambda - 6\mu + \frac{7}{6}, -8\lambda + 4\mu - \frac{1}{3}, 2\lambda - \mu + \frac{1}{18}\right\},$$

being λ *and* μ *free parameters.*

Proof. The BB-coefficients $c(x_i)$, $c(v_i)$, $c(u_{i+1})$ and $c(x_{i+1})$ of Qf relative to I_i are given by (3). They need to satisfy the C^1-conditions (4), as well as the exactness on $\mathbb{P}_3$. To this end, the BB-coefficients of Qm_k in I_i and those of m_k must be the same (Lemma 2). Those of Qm_k, $k = 0, \dots, 3$, are

$$\left(\beta_0 + \beta_1 + \beta_2 + \beta_3 + \beta_4, \gamma_0 + \gamma_1 + \gamma_2 + \gamma_3 + \gamma_4, \delta_0 + \delta_1 + \delta_2 + \delta_3 + \delta_4, \beta_0 + \beta_1 + \beta_2 + \beta_3 + \beta_4\right),$$
$$\left(-2\beta_0 - \beta_1 + \beta_3 + 2\beta_4, -2\gamma_0 - \gamma_1 + \gamma_3 + 2\gamma_4, -\delta_0 + \delta_2 + 2\delta_3 + 3\delta_4, -\beta_0 + \beta_2 + 2\beta_3 + 3\beta_4\right),$$
$$\left(4\beta_0 + \beta_1 + \beta_3 + 4\beta_4, 4\gamma_0 + \gamma_1 + \gamma_3 + 4\gamma_4, \delta_0 + \delta_2 + 4\delta_3 + 9\delta_4, \beta_0 + \beta_2 + 4\beta_3 + 9\beta_4\right),$$
$$\left(-8\beta_0 - \beta_1 + \beta_3 + 8\beta_4, -8\gamma_0 - \gamma_1 + \gamma_3 + 8\gamma_4, -\delta_0 + \delta_2 + 8\delta_3 + 27\delta_4, -\beta_0 + \beta_2 + 8\beta_3 + 27\beta_4\right).$$

Therefore, there are 5 equations ensuring the C^1-smoothness and 16 equations that guarantee the exactness on $\mathbb{P}_3$. In total, there are 21 equations and 15 unknowns. The general solution in the statement is determined by using a Computer Algebra System. □

The existence of two degrees of freedom allows additional conditions to be imposed on the masks. Since β is symmetric, one could require δ to be the symmetric mask of γ, i.e. $\delta_\ell = \gamma_{4-\ell}$, $\ell = 0, 1, 2$. This will be true if $\lambda = \mu - \frac{1}{36}$. This condition leads to the following masks:

$$\begin{aligned}
\beta_\mu &= \left(\mu - \frac{1}{36}, -4\mu + \frac{1}{9}, 6\mu + \frac{5}{6}, -4\mu + \frac{1}{9}, \mu - \frac{1}{36}\right),\\
\gamma_\mu &= \left(\mu, -4\mu - \frac{1}{9}, 6\mu + \frac{5}{6}, -4\mu + \frac{1}{3}, \mu - \frac{1}{18}\right),\\
\delta_\mu &= \left(\mu - \frac{1}{18}, -4\mu + \frac{1}{3}, 6\mu + \frac{5}{6}, -4\mu - \frac{1}{9}, \mu\right).
\end{aligned} \tag{5}$$

They produce the quasi-interpolation operator Q_μ defined as $Q_\mu[f] := Q_\mu f$ whose infinity norm is bounded by $U(\mu) := \max\left\{\|\beta\|_1, \|\gamma\|_1, \|\delta\|_1\right\}$. A possibility is to select the parameter μ consist of minimizing

$$U(\mu) = \frac{1}{18}\max\left\{5\,|1 - 36\mu| + 3\,|5 + 36\mu|,\ 6\,|1 - 12\mu| + 18\,|\mu| + |1 - 18\mu| + 2\,|1 + 36\mu| + 3\,|5 + 36\mu|\right\}.$$

It is a strictly convex function and attains its minimum value (equal to $\frac{11}{9}$) uniquely at $\mu_1 = -\frac{1}{36}$. Fig. 3 shows the objective function in a neighborhood of the point at which the minimum value is attained. The masks for this value of μ are

$$\beta_{\mu_1} = \left\{-\frac{1}{18}, \frac{2}{9}, \frac{2}{3}, \frac{2}{9}, -\frac{1}{18}\right\}, \quad \gamma_{\mu_1} = \left\{-\frac{1}{36}, 0, \frac{2}{3}, \frac{4}{9}, -\frac{1}{12}\right\}, \quad \delta_{\mu_1} = \left\{-\frac{1}{12}, \frac{4}{9}, \frac{2}{3}, 0, -\frac{1}{36}\right\}. \tag{6}$$

Alternatively, the free parameter μ can be chosen so that Q becomes an interpolating operator. This is achieved for $\mu_2 = \frac{1}{36}$. The masks in this case are

$$\beta_{\mu_2} = \{0, 0, 1, 0, 0\}, \quad \gamma_{\mu_2} = \left\{\frac{1}{36}, -\frac{2}{9}, 1, \frac{2}{9}, -\frac{1}{36}\right\}, \quad \delta_{\mu_2} = \left\{-\frac{1}{36}, \frac{2}{9}, 1, -\frac{2}{9}, \frac{1}{36}\right\}. \tag{7}$$

The following result holds.

Theorem 4. *For the masks given in (6) or (7) then*

(1) $Q_\mu f$ *is* C^1*-continuous,*
(2) $Q_\mu f = f$ *for all* $f \in \mathbb{P}_3$,
(3) $\left\|Q_\mu f - f\right\|_{\infty, I} = \mathcal{O}(h^4)$ *for all* $f \in C^4(I)$.

Proof. The result follows as a consequence of Proposition 1, Lemma 2 and Proposition 3 (see [14, Prop. 4.1]). □

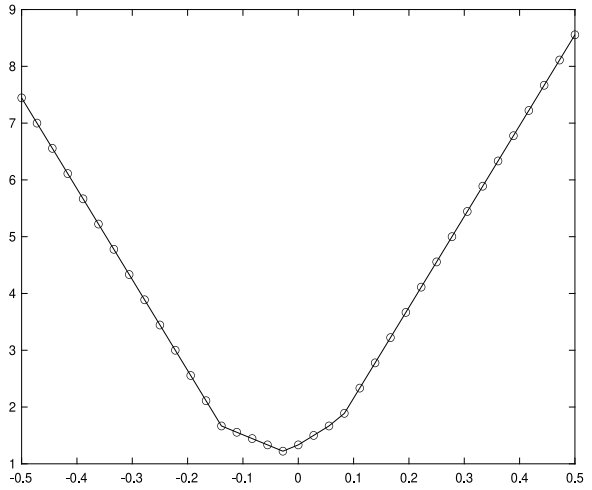

Fig. 3. Plot of the objective function.

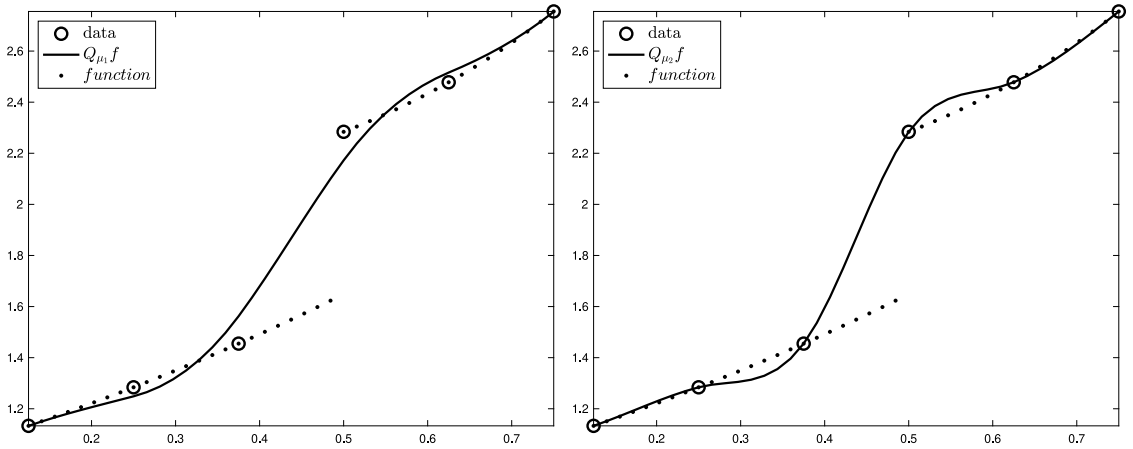

Fig. 4. Reconstructions of a discontinuous function (19) with Q_{μ_1} (left) and Q_{μ_2} (right).

In Fig. 4 we can see the reconstruction that we obtain from the function (19) with $\mu_1 = -\frac{1}{36}$ and $\mu_2 = \frac{1}{36}$.

An oscillation occurs around the discontinuity point, and it is clear that the magnitude of the overshoot and undershoot is lower in the case of quasi-interpolation, i.e. Q_{μ_1}. This happens, because in the setting of the BB-coefficients relative to the interval in which the discontinuity is located, values of a non-smooth stencil are used. In what follows, we will provide a non-linear improvement of the setting of these BB-coefficients based on the WENO approach.

3. WENO schemes with three points

The idea behind WENO is to split a large stencil into a number of small sub-stencils, and then associate a weight to each of them. The weight should override the use of the values in the associated stencil if there is a jump within it. To this end, we will write each of the three above masks as linear combinations of masks associated with stencils with three or four point values. More precisely, we will write the quasi-interpolant $Q_\mu f$ as a convex combination of several quasi-interpolants using stencils of fewer values than that of the quasi-interpolant $Q_\mu f$, i.e., we will determine three operators Q^ℓ, Q^c and Q^r defined from three sub-stencils of S_i, such that

$$Q_\mu f_{|_{I_i}} = \tau^\ell Q^\ell f_{|_{I_i}} + \tau^c Q^c f_{|_{I_i}} + \tau^r Q^r f_{|_{I_i}}, \tag{8}$$

with $\tau^\ell + \tau^c + \tau^r = 1$, $\tau^p \geq 0$ and $p = \ell, c, r$.

In fact, the WENO technique [2,3,19,21] is mainly based on defining

$$Q^\omega_\mu f_{|_{I_i}} = \omega^\ell_i Q^\ell_\mu f_{|_{I_i}} + \omega^c_i Q^c_\mu f_{|_{I_i}} + \omega^r_i Q^r_\mu f_{|_{I_i}} \tag{9}$$

where ω_i^p, $p = \ell, c, r$, has to be built so that if f is smooth, then $\omega_i^p \approx \tau^p$ and $Q_\mu^\omega f_{|_{I_i}} \approx Q_\mu f_{|_{I_i}}$. On the other hand, if f has a discontinuity at $(x_i, x_{i+1}]$ then $\omega_i^\ell \approx 1$, $\omega_i^p \approx 0$, $p = c, r$, and $Q_\mu^\omega f_{|_{I_i}} \approx Q_\mu^\ell f_{|_{I_i}}$, keeping the properties of the latter.

Unfortunately, this cannot be apply directly to the different polynomials $Q_\mu^p f_{|_{I_i}}$ because the BB-coefficients that we use to construct them depend on different stencils. What we do is to define

$$Q_\mu^\omega f_{|_{I_i}}(x) = w(x_i)\,\mathfrak{B}^i_{(3,0)}(x) + w(v_i)\,\mathfrak{B}^i_{(2,1)}(x) + c(u_{i+1})\,\mathfrak{B}^i_{(1,2)}(x) + w(x_{i+1})\,\mathfrak{B}^i_{(0,3)}(x), \tag{10}$$

where, for each i,

$$\begin{aligned} w(x_i) &= \omega_i^\ell < \beta^\ell, f(S_i^\ell) > + \omega_i^c < \beta^c, f(S_i^c) > + \omega_i^r < \beta^r, f(S_i^r) >,\\ w(v_i) &= \omega_i^\ell < \gamma^\ell, f(S_i^\ell) > + \omega_i^c < \gamma^c, f(S_i^c) > + \omega_i^r < \gamma^r, f(S_i^r) >,\\ w(u_i) &= \omega_i^\ell < \delta^\ell, f(S_i^\ell) > + \omega_i^c < \delta^c, f(S_i^c) > + \omega_i^r < \delta^r, f(S_i^r) >, \end{aligned}$$

with [2,3,19]

$$\alpha_i^p = \frac{\tau^p}{(\varepsilon + IS_i^p)^2} \quad \text{and} \quad \omega_i^p = \frac{\alpha_i^p}{\alpha_i^\ell + \alpha_i^c + \alpha_i^r}, \tag{11}$$

for $p = \ell, c, r$, where $\varepsilon = h^2$ and

$$\begin{aligned} IS_i^\ell &= \frac{13}{12}(f(x_{i-2}) - 2f(x_{i-1}) + f(x_i))^2 + \frac{1}{4}(f(x_{i-2}) - 4f(x_{i-1}) + 3f(x_i))^2,\\ IS_i^c &= \frac{13}{12}(f(x_{i-1}) - 2f(x_i) + f(x_{i+1}))^2 + \frac{1}{4}(f(x_{i-1}) - f(x_{i+1}))^2,\\ IS_i^r &= \frac{13}{12}(f(x_i) - 2f(x_{i+1}) + f(x_{i+2}))^2 + \frac{1}{4}(3f(x_i) - 4f(x_{i+1}) + f(x_{i+2}))^2. \end{aligned}$$

3.1. Interpolatory WENO

The stencil S_i can be divided into three sub-stencils $S_i^\ell := (x_{i-2}, x_{i-1}, x_i)$, $S_i^c = (x_{i-1}, x_i, x_{i+1})$ and $S_i^r = (x_i, x_{i+1}, x_{i+2})$. We are interested in defining masks leading to BB-coefficients providing C^1-cubic quasi-interpolants exact on some space $\mathbb{P}_d$. Of course, $d < 3$ because of the lowest number of point values used.

Problem 2. Consider the stencils S_i^p, where the symbol p refers to one of the labels ℓ, c and r. Then, find masks $\beta^p := (\beta_0^p, \beta_1^p, \beta_2^p)$, $\gamma^p := (\gamma_0^p, \gamma_1^p, \gamma_2^p)$ and $\delta^p := (\delta_0^p, \delta_1^p, \delta_2^p)$ such that the quasi-interpolant $Q^p f$ defined on each sub-interval I_i according to (2) with BB-coefficients

$$c(u_i) = \langle \delta^p, f(S_i^p)\rangle, \quad c(x_i) = \langle \beta^p, f(S_i^p)\rangle, \quad c(v_i) =< \gamma^p, f(S_i^p) >$$

is C^1-continuous and $Q^p f = f$ for all $f \in \mathbb{P}_2$.

Using the same approach used to solve Problem 1, the following result holds.

Proposition 5. *Problem 2 has a unique solution provided by the following masks*

1. *For the left stencil S_i^ℓ,*

$$\beta_{\mu_2}^\ell = (0,0,1), \quad \gamma_{\mu_2}^\ell = \left(\frac{1}{6}, -\frac{2}{3}, \frac{3}{2}\right), \quad \delta_{\mu_2}^\ell = \left(-\frac{1}{6}, \frac{2}{3}, \frac{1}{2}\right).$$

2. *For the centered stencil S_i^c,*

$$\beta_{\mu_2}^c = (0,1,0), \quad \gamma_{\mu_2}^c = \left(-\frac{1}{6}, 1, \frac{1}{6}\right), \quad \delta_{\mu_2}^c = \left(\frac{1}{6}, 1, -\frac{1}{6}\right).$$

3. *For the right stencil S_i^r,*

$$\beta_{\mu_2}^r = (1,0,0), \quad \gamma_{\mu_2}^r = \left(\frac{1}{2}, \frac{2}{3}, -\frac{1}{6}\right), \quad \delta_{\mu_2}^r = \left(\frac{3}{2}, -\frac{2}{3}, \frac{1}{6}\right).$$

Proof. The proof is done only for the case of the masks associated with the left stencil being similar for the other cases. $Q^\ell f$ is C^1-continuous if, and only if, $\beta_k^\ell - \frac{\gamma_k^\ell}{2} - \frac{\delta_k^\ell}{2} = 0$, $k = 0, 1, 2$.

The quasi-interpolant $Q^\ell f$ should be exact on $\mathbb{P}_2$, i.e. $Q^\ell \left(\frac{x - x_i}{h}\right)^k = \left(\frac{x - x_i}{h}\right)^k$, $k = 0, 1, 2$. This is achieved if

$$\begin{aligned} &\beta_0^\ell + \beta_1^\ell + \beta_2^\ell = 1, \quad \gamma_0^\ell + \gamma_1^\ell + \gamma_2^\ell = 1, \quad \delta_0^\ell + \delta_1^\ell + \delta_2^\ell = 1, \quad \beta_0^\ell + \beta_1^\ell + \beta_2^\ell = 1,\\ &2\beta_0^\ell + \beta_1^\ell + 1 = 0, \quad 2\gamma_0^\ell + \gamma_1^\ell + 1 = 0, \quad \delta_0^\ell + 1 - \delta_2^\ell = 0, \quad \beta_0^\ell - \beta_2^\ell + 1 = 0,\\ &4\beta_0^\ell + \beta_1^\ell = 1, \quad 4\gamma_0^\ell + \gamma_1^\ell = 1, \quad \delta_0^\ell + \delta_2^\ell = 1, \quad \beta_0^\ell + \beta_2^\ell = 1. \end{aligned}$$

It results a linear system of 14 equations, 3 guaranteeing C^1-continuity and 11 ensuring the optimal order. The main matrix of this system is non-singular, which means that there is a unique solution, which is provided in the statement. □

$Q_{\mu_2} f$ defined according (2) from the masks given in (7) can be written as a convex combination of $Q^{\ell}_{\mu_2} f$, $Q^{c}_{\mu_2} f$ and $Q^{r}_{\mu_2} f$ as:

$$Q_{\mu_2} f = \frac{1}{6}\left(Q^{\ell}_{\mu_2} f + 4Q^{c}_{\mu_2} f + Q^{r}_{\mu_2} f\right).$$

Theorem 6. *If we take $\tau^{\ell} = \tau^{r} = 1/6$, $\tau^{c} = 4/6$ in (11) and define*

$$Q^{\omega}_{\mu_2} f_{|_{I_i}}(x) = w\left(x_i\right)\mathfrak{B}^{i}_{(3,0)}(x) + w\left(v_i\right)\mathfrak{B}^{i}_{(2,1)}(x) + w\left(u_{i+1}\right)\mathfrak{B}^{i}_{(1,2)}(x) + w\left(x_{i+1}\right)\mathfrak{B}^{i}_{(0,3)}(x), \tag{12}$$

then, if f is smooth, we have

- $Q^{\omega}_{\mu_2} f$ *is C^1-continuous,*
- $Q^{\omega}_{\mu_2} f = f$ *for all $f \in \mathbb{P}_2$,*
- $\left\|Q^{\omega}_{\mu_2} f - f\right\|_{\infty,I} = \mathcal{O}(h^4)$ *for all $f \in C^4(I)$,*

and if f has a discontinuity at (x_{i-1}, x_i) then

- $Q^{\omega}_{\mu_2} f$ *is C^1-continuous,*
- $\left\|Q^{\omega}_{\mu_2} f - f\right\|_{\infty,[a,x_{i-1}]\cup[x_i,b]} = \mathcal{O}(h^3)$.

Proof. In both cases, $Q^{\omega}_{\mu_2} f$ is C^1 smooth, since is just a combination of three smooth operators. Thus,

$$\begin{aligned}\left\|Q^{\omega}_{\mu_2} f - f\right\|_{\infty,I} &= \left\|Q^{\omega}_{\mu_2} f - Q_{\mu_2} f + Q_{\mu_2} f - f\right\|_{\infty,I}\\ &\le \left\|Q^{\omega}_{\mu_2} f - Q_{\mu_2} f\right\|_{\infty,I} + \left\|Q_{\mu_2} f - f\right\|_{\infty,I}.\end{aligned}$$

By construction, if f is smooth, then $\left\|Q^{\omega}_{\mu_2} f - Q_{\mu_2} f\right\|_{\infty,I} = \mathcal{O}(h^4)$, and by Theorem 4, we have $\left\|Q_{\mu} f - f\right\|_{\infty,I} = \mathcal{O}(h^4)$, which proves that $\left\|Q^{\omega}_{\mu_2} f - f\right\|_{\infty,I} = \mathcal{O}(h^4)$. This not ensures that $Q^{\omega}_{\mu_2} p = p$, $p \in \mathbb{P}_3$. Although, the operator $Q^{\omega}_{\mu_2}$ is a combination of three operator that are exact on $\mathbb{P}_2$, which proves the statements in the case that f is smooth.

If f is discontinuous at $\bar{x} \in (x_{i-1}, x_i)$, then the BB-coefficients related to the intervals I_{i+j}, $j = -2, -1, 0, 1$, will be affected. Namely, at maximum two weights (ω^p) should be ≈ 0, and then

$$\left\|Q^{\omega}_{\mu_2} f - Q_{\mu_2} f\right\|_{\infty,I_i} = \max\left\{\left\|Q^{\ell}_{\mu_2} f - Q_{\mu_2} f\right\|_{\infty,J_i}, \left\|Q^{c}_{\mu_2} f - Q_{\mu_2} f\right\|_{\infty,J_i}, \left\|Q^{r}_{\mu_2} f - Q_{\mu_2} f\right\|_{\infty,J_i}\right\},$$

being $J_i = [a, x_{i-1}] \cup [x_i, b]$. Moreover, $\left\|Q^{p}_{\mu_2} f - Q_{\mu_2} f\right\|_{\infty,R} = \mathcal{O}(h^3)$, $p = \ell, c, r$, in smooth regions R, which concludes the proof. □

In the case of quasi-interpolants $Q^{p}_{\mu} f$, $p = \ell, c, r$, exact on $\mathbb{P}_2$, we get masks without free parameters so that we cannot write $Q_{\mu} f$ as a combination of $Q^{p}_{\mu} f$ for any μ. This can only be achieved in the case of $\mu_2 = \frac{1}{36}$. Therefore, we will consider operators Q^{p}_{μ} that are exact only on $\mathbb{P}_1$.

3.2. Quasi-interpolatory WENO

Taking into account the previous comment, we will consider now operators Q^p exacts only in $\mathbb{P}_1$.

Proposition 7. *Consider again the stencils S^{p}_{i}, $p = \ell, c, r$. Define on each sub-interval I_i the operators Q^p according to (2) with BB-coefficients*

$$c\left(u_i\right) = \langle \delta^p, f(S^{p}_{i})\rangle, \quad c\left(x_i\right) = \langle \beta^p, f(S^{p}_{i})\rangle, \quad c\left(v_i\right) = \langle \gamma^p, f(S^{p}_{i})\rangle.$$

Then, $Q^p f$ are C^1-continuous and $Q^p f = f$ for all $f \in \mathbb{P}_1$ if, and only if, the masks are as follows:

1. *for the left stencil S^{ℓ}_{i},*

$$\beta^{\ell} = \left(\alpha^{\ell}, -2\alpha^{\ell}, \alpha^{\ell} + 1\right),\ \gamma^{\ell} = \left(\rho^{\ell}, -2\rho^{\ell} - \frac{1}{3}, \rho^{\ell} + \frac{4}{3}\right),\ \delta^{\ell} = \left(2\alpha^{\ell} - \rho^{\ell}, -4\alpha^{\ell} + 2\rho^{\ell} + \frac{1}{3}, 2\alpha^{\ell} - \rho^{\ell} + \frac{2}{3}\right);$$

2. *for the centered stencil S^{c}_{i},*

$$\beta^{c} = (\alpha^{c}, 1 - 2\alpha^{c}, \alpha^{c}),\ \gamma^{c} = \left(\rho^{c}, \frac{2}{3} - 2\rho^{c}, \rho^{c} + \frac{1}{3}\right),\ \delta^{c} = \left(2\alpha^{c} - \rho^{c}, -4\alpha^{c} + 2\rho^{c} + \frac{4}{3}, 2\alpha^{c} - \rho^{c} - \frac{1}{3}\right);$$

3. *for the right stencil S^{r}_{i},*

$$\beta^{r} = (\alpha^{r}, 2 - 2\alpha^{r}, \alpha^{r} - 1),\ \gamma^{r} = \left(\rho^{r}, \frac{5}{3} - 2\rho^{r}, \rho^{r} - \frac{2}{3}\right),\ \delta^{r} = \left(2\alpha^{r} - \rho^{r}, -4\alpha^{r} + 2\rho^{r} + \frac{7}{3}, 2\alpha^{r} - \rho^{r} - \frac{4}{3}\right),$$

α^p and ρ^p being free parameters.

The BB-coefficients of the quasi-interpolant Qf defined on I_i from the stencil S_i and the masks given by (6) are

$$c\left(x_i\right)=\langle\beta_{\mu_1},f(S_i)\rangle,\ c\left(v_i\right)=\langle\gamma_{\mu_1},f(S_i)\rangle,\ c\left(u_{i+1}\right)=<\delta_{\mu_1},f(S_{i+1})>\ \text{ and }\ c\left(x_{i+1}\right)=<\beta_{\mu_1},f(S_{i+1})>.$$

We want to express $Q_\mu f$ in terms of the masks in Proposition 7. Then for $\mu=\mu_1$ we look for coefficients α^p and ρ^p, $p=\ell,c,r$, such that

$$\begin{aligned}
c\left(x_i\right)&=\langle\beta_{\mu_1},f(S_i)\rangle=\frac{1}{3}\left(\langle\beta^\ell,f(S_i^\ell)\rangle+<\beta^c,f(S_i^c)>+\langle\beta^r,f(S_i^r)\rangle\right),\\
c(v_i)&=\langle\gamma_{\mu_1},f(S_i)\rangle=\frac{1}{3}\left(<\gamma^\ell,f(S_i^\ell)>+\langle\gamma^c,f(S_i^c)\rangle+<\gamma^r,f(S_i^r)>\right),\\
c(u_i)&=\langle\delta_{\mu_1},f(S_i)\rangle=\frac{1}{3}\left(<\delta^\ell,f(S_i^\ell)>+\langle\delta^c,f(S_i^c)\rangle+<\delta^r,f(S_i^r)>\right).
\end{aligned}\tag{13}$$

It is straightforward to prove the following result.

Proposition 8. *There are unique values α^p and ρ^p, $p=\ell,c,r$, such that equalities (13) are satisfied. They are*

$$\alpha^\ell=-\frac{1}{6},\quad \alpha^c=\frac{1}{3},\quad \alpha^r=\frac{5}{6},\quad \rho^\ell=-\frac{1}{12},\quad \rho^c=\frac{1}{6},\quad \rho^r=\frac{5}{12}.$$

The coefficients in Proposition 8 give the following masks for the interpolants Q^pf, $p=\ell,c,r$, defined in Proposition 7:

$$\begin{aligned}
Q^\ell f:&\quad \beta^\ell=\left(-\frac{1}{6},\frac{1}{3},\frac{5}{6}\right),\quad \gamma^\ell=\left(-\frac{1}{12},-\frac{1}{6},\frac{5}{4}\right),\quad \delta^\ell=\left(-\frac{1}{4},\frac{5}{6},\frac{5}{12}\right),\\
Q^cf:&\quad \beta^c=\left(\frac{1}{3},\frac{1}{3},\frac{1}{3}\right),\quad \gamma^c=\left(\frac{1}{6},\frac{1}{3},\frac{1}{2}\right),\quad \delta^c=\left(\frac{1}{2},\frac{1}{3},\frac{1}{6}\right),\\
Q^rf:&\quad \beta^r=\left(\frac{5}{6},\frac{1}{3},-\frac{1}{6}\right),\quad \gamma^r=\left(\frac{5}{12},\frac{5}{6},-\frac{1}{4}\right),\quad \delta^r=\left(\frac{5}{4},-\frac{1}{6},-\frac{1}{12}\right).
\end{aligned}$$

These quasi-interpolants are exact on $\mathbb{P}_1$. However, the parameters have been calculated in such a way that the initial quasi-interpolant Q_{μ_1} defined from the masks in (6), which is exact on $\mathbb{P}_3$, is expressed from them, i.e., $Q_{\mu_1}f=\tau^\ell Q^\ell f+\tau^c Q^c f+\tau^r Q^r f$. In the next result, we provide the explicit values of the parameters τ^ℓ, τ^c and τ^r.

Theorem 9. *If we take $\tau^\ell=\tau^c=\tau^r=1/3$ in (11) and define*

$$Q^\omega_{\mu_1}f_{|_{I_i}}(x)=w\left(x_i\right)\mathfrak{B}^i_{(3,0)}(x)+w\left(v_i\right)\mathfrak{B}^i_{(2,1)}(x)+w\left(u_{i+1}\right)\mathfrak{B}^i_{(1,2)}(x)+w\left(x_{i+1}\right)\mathfrak{B}^i_{(0,3)}(x)\tag{14}$$

then, if f is smooth, we have

- *$Q^\omega_{\mu_1}f$ is C^1-continuous,*
- *$Q^\omega_{\mu_1}f=f$ for all $f\in\mathbb{P}_1$,*
- *$\left\|Q^\omega_{\mu_1}f-f\right\|_{\infty,I}=\mathcal{O}(h^4)$ for all $f\in C^4(I)$,*

and if f has a discontinuity at (x_{i-1},x_i) then

- *$Q^\omega_{\mu_1}f$ is C^1-continuous,*
- *$\left\|Q^\omega_{\mu_1}f-f\right\|_{\infty,[a,x_{i-1}]\cup[x_i,b]}=\mathcal{O}(h^2)$.*

Proof. Similar arguments as in Theorem 6 can be applied, however, in this case the quasi-interpolants $Q^p_{\mu_1}$, $p=\ell,c,r$, are exact on $\mathbb{P}_1$, meaning that $\left\|Q^p_{\mu_1}f-Q_{\mu_1}f\right\|_{\infty,R}=\mathcal{O}(h^2)$ in smooth regions R. □

In Fig. 5 we see the reconstruction that we obtain with the WENO techniques of this section.

The BB-coefficients in (13) are specifically calculated under the condition $\mu=\mu_1=-\frac{1}{36}$. However, this computation can be extended to encompass any arbitrary free parameter μ, resulting in the derivation of the masks β_μ, γ_μ, and δ_μ, as formally defined in (5).

$$\begin{aligned}
c\left(x_i\right)&=\langle\beta_\mu,f(S_i)\rangle=a\left(<\beta^\ell_\mu,f(S_i^\ell)>+\langle\beta^c_\mu,f(S_i^c)\rangle+<\beta^r_\mu,f(S_i^r)>\right),\\
c(v_i)&=\langle\gamma_\mu,f(S_i)\rangle=(1-2a)\left(<\gamma^\ell_\mu,f(S_i^\ell)>+\langle\gamma^c_\mu,f(S_i^c)\rangle+<\gamma^r_\mu,f(S_i^r)>\right),\\
c(u_i)&=\langle\delta_\mu,f(S_i)\rangle=a\left(<\delta^\ell_\mu,f(S_i^\ell)>+\langle\delta^c_\mu,f(S_i^c)\rangle+<\delta^r_\mu,f(S_i^r)>\right).
\end{aligned}\tag{15}$$

It is straightforward to prove the following result.

Proposition 10. *There exist unique values α^p and ρ^p such that equalities (15) are satisfied. They are*

$$\alpha^\ell=\frac{36\mu-1}{36a},\ \alpha^c=\frac{36\mu-1}{18(2a-1)},\ \alpha^r=\frac{36\mu-1+36a}{36a},\ \rho^\ell=\frac{\mu}{a},\ \rho^c=\frac{1+18\nu-3a}{9(2a-1)},\ \rho^r=\frac{18\mu-1+12a}{18a}.$$

Next, we will split the stencil S_i into just two sub-stencils, which is maybe lead to a good accuracy, but as we will show it is not appropriate, because we cannot avoid using the values in a non-smooth stencil, and that is due to the fact that the two sub-stencils overlap.

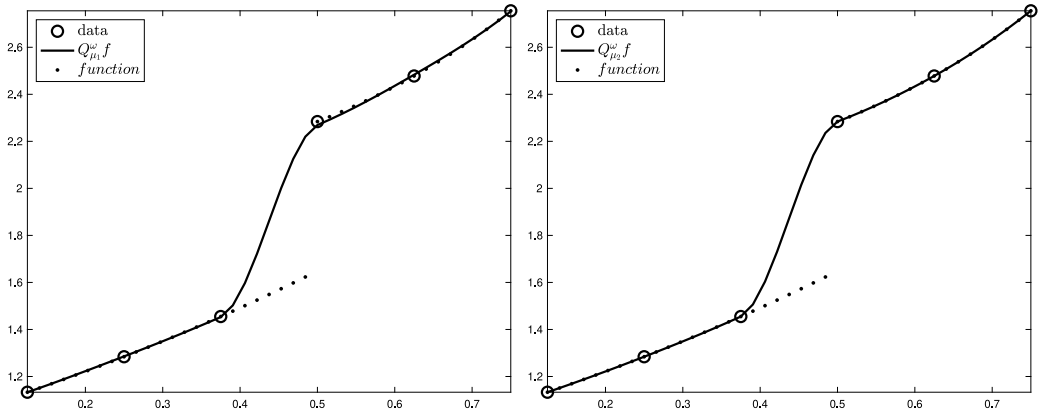

Fig. 5. Reconstructions of a discontinuous function (19) with $Q^{\omega}_{\mu_1}$ (left) and $Q^{\omega}_{\mu_2}$ (right).

4. WENO with four values

In the previous section a specific quasi-interpolant has been constructed to approximate discontinuous functions by adopting a WENO procedure. The stencil has been decomposed into three sub-stencils, from which three quasi-interpolants are defined and combined to form the approximant we are looking for. It is natural to ask whether such a stencil could be decomposed into two sub-stencils and obtain a spline approximant with good properties. To do so, let us define

$$\overline{S}_i^{\ell} = \left(x_{i-2}, x_{i-1}, x_i, x_{i+1}\right) \quad \text{and} \quad \overline{S}_i^{r} = \left(x_{i-1}, x_i, x_{i+1}, x_{i+2}\right).$$

From them, two quasi-interpolants $\overline{Q}^{\ell} f$ and $\overline{Q}^{r} f$ of the form (1) are constructed in such a way that they are C^1-continuous and the quadratic/cubic polynomials are reproduced. As before, their BB-coefficients will be of the form

$$c\left(x_i\right) = \langle \beta^p, f(\overline{S}_i^p)\rangle, \quad c\left(v_i\right) = \langle \gamma^p, f(\overline{S}_i^p)\rangle \quad \text{and} \quad c\left(u_i\right) = \langle \delta^p, f(\overline{S}_i^p)\rangle$$

for labels p equal to ℓ and r.

In what follows, we start by providing two interpolating cubic splines $\overline{Q}_{\mu}^{\ell} f$ and $\overline{Q}_{\mu}^{r} f$ which reproduce cubic polynomials and they meet

$$Q_{\mu} f = \tau \overline{Q}_{\mu}^{\ell} f + (1-\tau)\, \overline{Q}_{\mu}^{r} f. \tag{16}$$

Proposition 11. *The quasi-interpolants $\overline{Q}_{\mu}^{\ell} f$ and $\overline{Q}_{\mu}^{r} f$ are C^1-continuous and reproduce cubic polynomials if, and only if,*

$$\beta^{\ell} = (0,0,1,0), \quad \gamma^{\ell} = \left(\frac{1}{18}, -\frac{1}{3}, \frac{7}{6}, \frac{1}{9}\right), \quad \delta^{\ell} = \left(-\frac{1}{18}, \frac{1}{3}, \frac{5}{6}, -\frac{1}{9}\right),$$

and

$$\beta^{r} = (0,1,0,0), \quad \gamma^{r} = \left(-\frac{1}{9}, \frac{5}{6}, \frac{1}{3}, -\frac{1}{18}\right), \quad \delta^{r} = \left(\frac{1}{9}, \frac{7}{6}, -\frac{1}{3}, \frac{1}{18}\right).$$

The next result shows the relation between Q_{μ}, $\overline{Q}_{\mu}^{\ell}$ and $\overline{Q}_{\mu}^{r}$.

Proposition 12. *Eq. (16) holds if, and only if, $\tau = \frac{1}{2}$ and $\mu = \mu_2 = \frac{1}{36}$.*

Proof. The proof is straightforward, simply substitute τ and μ by their values and the result follows. □

Theorem 13. *If we take $\tau^{\ell} = \tau^{r} = 1/2$, $\tau^{c} = 0$ in (11) where, now,*

$$\begin{aligned}
\widehat{IS}_i^{\ell} &= \frac{1}{2}(f(x_{i-2}) - 2f(x_{i-1}) + f(x_i))^2 + \frac{1}{2}(f(x_{i-1}) - 2f(x_i) + f(x_{i+1}))^2 \\
&\quad + (f(x_{i-2}) - 3f(x_{i-1}) + 3f(x_i) - f(x_{i+1}))^2, \\
\widehat{IS}_i^{r} &= \frac{1}{2}(f(x_{i-1}) - 2f(x_i) + f(x_{i+1}))^2 + \frac{1}{2}(f(x_i) - 2f(x_{i+1}) + f(x_{i+2}))^2 \\
&\quad + (f(x_{i-1}) - 3f(x_i) + 3f(x_{i+1}) - f(x_{i+2}))^2,
\end{aligned}$$

and define

$$\widehat{Q}^{\omega}_{\mu_2} f_{|_{I_i}}(x) = w\left(x_i\right) \mathfrak{B}^i_{(3,0)}(x) + w\left(v_i\right) \mathfrak{B}^i_{(2,1)}(x) + w\left(u_{i+1}\right) \mathfrak{B}^i_{(1,2)}(x) + w\left(x_{i+1}\right) \mathfrak{B}^i_{(0,3)}(x),$$

where, for each i,

$$
\begin{aligned}
w\left(x_i\right) &= \omega_i^{\ell} \ < \beta^{\ell}, f(\widehat{S}_i^{\ell}) > + \omega_i^{r} \ \langle \beta^{r}, f(\widehat{S}_i^{r}) \rangle, \\
w\left(v_i\right) &= \omega_i^{\ell} \ < \gamma^{\ell}, f(\widehat{S}_i^{\ell}) > + \omega_i^{r} \ \langle \gamma^{r}, f(\widehat{S}_i^{r}) \rangle, \\
w\left(u_i\right) &= \omega_i^{\ell} \ < \delta^{\ell}, f(\widehat{S}_i^{\ell}) > + \omega_i^{r} \ \langle \delta^{r}, f(\widehat{S}_i^{r}) \rangle,
\end{aligned}
$$

then, if f is smooth, it holds

- $\widehat{Q}^{\omega}_{\mu_2} f$ *is* C^1*-continuous,*
- $\widehat{Q}^{\omega}_{\mu_2} f = f$ *for all* $f \in \mathbb{P}_3$*,*
- $\left\| \widehat{Q}^{\omega}_{\mu_2} f - f \right\|_{\infty, I}$ *for all* $f \in C^4(I)$*,*

and if f has a discontinuity at (x_{i-1}, x_i) *then*

- $\widehat{Q}^{\omega}_{\mu_2} f$ *is* C^1*-continuous,*
- $\left\| \widehat{Q}^{\omega}_{\mu_2} f - f \right\|_{\infty, [a, x_{i-2}] \cup [x_i, b]} = \mathcal{O}(h^4)$.

Proof. The claims in the case that f is smooth follow from the fact that both operators $\overline{Q}^{\ell}_{\mu}$ and $\overline{Q}^{r}_{\mu}$ are exact on $\mathbb{P}_3$.

If f has a jump $\bar{x} \in [x_{i-1}, x_i]$, then only the BB-coefficients related to the domain points x_i, u_i, and v_i will be affected. For the BB-coefficients associated with the rest of domain points in D, at least one operator $\overline{Q}^{\ell}_{\mu}$ and/or $\overline{Q}^{r}_{\mu}$ should be used to compute them. Which leads to an accuracy of order 4. □

As shown in the last result, Eq. (16) fulfills only in the case of $\mu = \frac{1}{36}$, to get a large variety of possible values of μ, we may consider that the operators $\overline{Q}^{\ell}$ and $\overline{Q}^{r}$ are of near-optimal order, i.e. instead of reproducing cubic polynomials we will assume that they only reproduce quadratic polynomials.

Proposition 14. *The quasi-interpolants* $\overline{Q}^{\ell} f$ *and* $\overline{Q}^{r} f$ *are* C^1*-continuous and reproduce quadratic polynomials if, and only if,*

$$
\begin{aligned}
\beta^{\ell} &= \left(\alpha^{\ell}, -3\alpha^{\ell}, 3\alpha^{\ell} + 1, -\alpha^{\ell}\right), \\
\gamma^{\ell} &= \left(\rho^{\ell}, -3\rho^{\ell} - \frac{1}{6}, 3\rho^{\ell} + 1, \frac{1}{6} - \rho^{\ell}\right), \\
\delta^{\ell} &= \left(2\alpha^{\ell} - \rho^{\ell}, -6\alpha^{\ell} + 3\rho^{\ell} + \frac{1}{6}, 6\alpha^{\ell} - 3\rho^{\ell} + 1, -2\alpha^{\ell} + \rho^{\ell} - \frac{1}{6}\right),
\end{aligned}
$$

and

$$
\begin{aligned}
\beta^{r} &= \left(\alpha^{r}, 1 - 3\alpha^{r}, 3\alpha^{r}, -\alpha^{r}\right), \\
\gamma^{r} &= \left(\rho^{r}, \frac{1}{2} - 3\rho^{r}, 3\rho^{r} + \frac{2}{3}, -\rho^{r} - \frac{1}{6}\right), \\
\delta^{r} &= \left(2\alpha^{r} - \rho^{r}, -6\alpha^{r} + 3\rho^{r} + \frac{3}{2}, 6\alpha^{r} - 3\rho^{r} - \frac{2}{3}, -2\alpha^{r} + \rho^{r} + \frac{1}{6}\right),
\end{aligned}
$$

where α^{ℓ}*,* α^{r}*,* ρ^{ℓ} *and* ρ^{r} *are free parameters.*

The following result holds.

Proposition 15. *Eq. (16) holds if, and only if,*

$$
\mu = (\tau - 1)\alpha^{r} + \frac{1}{36}, \quad \alpha^{\ell} = \frac{(\tau - 1)\alpha^{r}}{\tau}, \quad \rho^{\ell} = \frac{36(\tau - 1)\alpha^{r} + 1}{36\tau}, \quad \rho^{r} = \alpha^{r} + \frac{5 - 6\tau}{36(\tau - 1)}, \tag{17}
$$

or

$$
\mu = \frac{\tau + 1}{36}, \quad \alpha^{\ell} = \frac{1}{36}, \quad \alpha^{r} = \frac{\tau}{36(\tau - 1)}, \quad \rho^{\ell} = \frac{\tau + 1}{36\tau}, \quad \rho^{r} = -\frac{5}{36}. \tag{18}
$$

Taking $\tau = 1/2$ and $\mu = \mu_1 = -1/36$ in (17), we obtain the masks

$$
\begin{aligned}
\beta^{\ell} &= \left(-\frac{1}{9}, \frac{1}{3}, \frac{2}{3}, \frac{1}{9}\right), \quad \gamma^{\ell} = \left(-\frac{1}{18}, 0, \frac{5}{6}, \frac{2}{9}\right), \quad \delta^{\ell} = \left(-\frac{1}{6}, \frac{2}{3}, \frac{1}{2}, 0\right), \\
\beta^{r} &= \left(\frac{1}{9}, \frac{2}{3}, 0, -\frac{1}{9}\right), \quad \gamma^{r} = \left(0, \frac{1}{2}, \frac{2}{3}, -\frac{1}{6}\right), \quad \delta = \left(\frac{2}{9}, \frac{5}{6}, 0, -\frac{1}{18}\right).
\end{aligned}
$$

Now, taking $\tau = 1/2$ in (18), we obtain $\mu_3 = \frac{1}{24}$

$$
\begin{aligned}
\beta^{\ell} &= \left(\frac{1}{36}, -\frac{1}{12}, \frac{13}{12}, -\frac{1}{36}\right), \quad \gamma^{\ell} = \left(\frac{1}{12}, -\frac{5}{12}, \frac{5}{4}, \frac{1}{12}\right), \quad \delta^{\ell} = \left(-\frac{1}{36}, \frac{1}{4}, \frac{11}{12}, -\frac{5}{36}\right), \\
\beta^{r} &= \left(-\frac{1}{36}, \frac{13}{12}, -\frac{1}{12}, \frac{1}{36}\right), \quad \gamma^{r} = \left(-\frac{5}{36}, \frac{11}{12}, \frac{1}{4}, -\frac{1}{36}\right), \quad \delta^{r} = \left(\frac{1}{12}, \frac{5}{4}, -\frac{5}{12}, \frac{1}{12}\right).
\end{aligned}
$$

Theorem 16. *If we take the masks given in Propositions 14 and 15 and define $\widehat{Q}_\mu^\omega$ using the WENO strategy like in Theorem 13, if f is smooth, we have*

- $\widehat{Q}_\mu^\omega f$ *is* C^1*-continuous,*
- $\widehat{Q}_\mu^\omega f = f$ *for all* $f \in \mathbb{P}_2$,
- $\left\| \widehat{Q}_\mu^\omega f - f \right\|_{\infty,I} = \mathcal{O}(h^4)$ *for all* $f \in C^4(I)$,

and if f has a discontinuity at (x_{i-1}, x_i) then

- $\widehat{Q}_\mu^\omega f$ *is* C^1*-continuous,*
- $\left\| \widehat{Q}_\mu^\omega f - f \right\|_{\infty,[a,x_{i-2}]\cup[x_i,b]} = \mathcal{O}(h^3)$.

Proof. The proof is similar to that of Theorem 13. □

5. ENO with four points

The use of 4-valued sub-stencils is not suitable, because it may be that the discontinuity occurs for example between the points x_i and x_{i+1}, in this case, the two operators $\overline{Q}_\mu^\ell$ and $\overline{Q}_\mu^r$ become affected by the discontinuity. Therefore, it is better to apply, in case one wants to use four values in each sub-stencil, ENO technique with four points on the right and four points on the left.

In this section we consider two stencils of four points that are not centered at x_i. Define,

$$\overline{S}_i^\ell = \{x_{i-3}, x_{i-2}, x_{i-1}, x_i\}, \quad \overline{S}_i^r = \{x_i, x_{i+1}, x_{i+2}, x_{i+3}\}.$$

Again consider two quasi-interpolants $\overline{Q}_\mu^\ell f$ and $\overline{Q}_\mu^r f$ of the form (1) such that both quasi-interpolants are C^1-continuous and reproduce cubic polynomials. More precisely, their BB-coefficients will be of the form:

$$c(x_i) = \langle \beta^p, f(\overline{S}_i^p)\rangle, \quad c(u_i) = \langle \delta^p, f(\overline{S}_i^p)\rangle \text{ and } c(v_i) = \langle \gamma^p, f(\overline{S}_i^p)\rangle, \qquad p = \ell, r.$$

Proposition 17. *The quasi-interpolant $\overline{Q}_\mu^\ell f$, resp. $\overline{Q}_\mu^r f$, is C^1-continuous and reproduce cubic polynomials if and only if:*

$$\beta^\ell = \{0,0,0,1\}, \quad \gamma^\ell = \left\{-\frac{1}{9}, \frac{1}{2}, -1, \frac{29}{18}\right\}, \quad \delta^\ell = \left\{\frac{1}{9}, -\frac{1}{2}, 1, \frac{7}{18}\right\},$$

resp.

$$\beta^r = \{1,0,0,0\}, \quad \gamma^r = \left\{\frac{7}{18}, 1, -\frac{1}{2}, \frac{1}{9}\right\}, \quad \delta^r = \left\{\frac{29}{18}, -1, \frac{1}{2}, -\frac{1}{9}\right\}.$$

Proof. The proof runs as in Proposition 3. □

Theorem 18. *If we define*

$$\bar{Q}_\mu^e f|_{I_i}(x) = w(x_i)\,\mathfrak{B}^i_{(3,0)}(x) + w(v_i)\,\mathfrak{B}^i_{(2,1)}(x) + c(u_{i+1})\,\mathfrak{B}^i_{(1,2)}(x) + w(x_{i+1})\,\mathfrak{B}^i_{(0,3)}(x),$$

where, for each i,

$$\begin{aligned}
w(x_i) &= (\overline{IS}_i^\ell < \overline{IS}_i^r)\,\langle \beta^\ell, \overline{S}_i^\ell\rangle + (\overline{IS}_i^\ell \geq \overline{IS}_i^r)\,\langle \beta^r, \overline{S}_i^r\rangle,\\
w(v_i) &= (\overline{IS}_i^\ell < \overline{IS}_i^r)\,\langle \gamma^\ell, \overline{S}_i^\ell\rangle + (\overline{IS}_i^\ell \geq \overline{IS}_i^r)\,\langle \gamma^r, \overline{S}_i^r\rangle,\\
w(u_i) &= (\overline{IS}_i^\ell < \overline{IS}_i^r)\,\langle \delta^\ell, \overline{S}_i^\ell\rangle + (\overline{IS}_i^\ell \geq \overline{IS}_i^r)\,\langle \delta^r, \overline{S}_i^r\rangle,
\end{aligned}$$

where [3,21]

$$\begin{aligned}
\overline{IS}_i^\ell &= \frac{1}{2}(f(x_{i-3}) - 2f(x_{i-2}) + f(x_{i-1}))^2 + \frac{1}{2}(f(x_{i-2}) - 2f(x_{i-1}) + f(x_i))^2\\
&\quad + (f(x_{i-3}) - 3f(x_{i-2}) + 3f(x_{i-1}) - f(x_i))^2,\\
\overline{IS}_i^r &= \frac{1}{2}(f(x_i) - 2f(x_{i+1}) + f(x_{i+2}))^2 + \frac{1}{2}(f(x_{i+1}) - 2f(x_{i+2}) + f(x_{i+3}))^2\\
&\quad + (f(x_i) - 3f(x_{i+1}) + 3f(x_{i+2}) - f(x_{i+3}))^2,
\end{aligned}$$

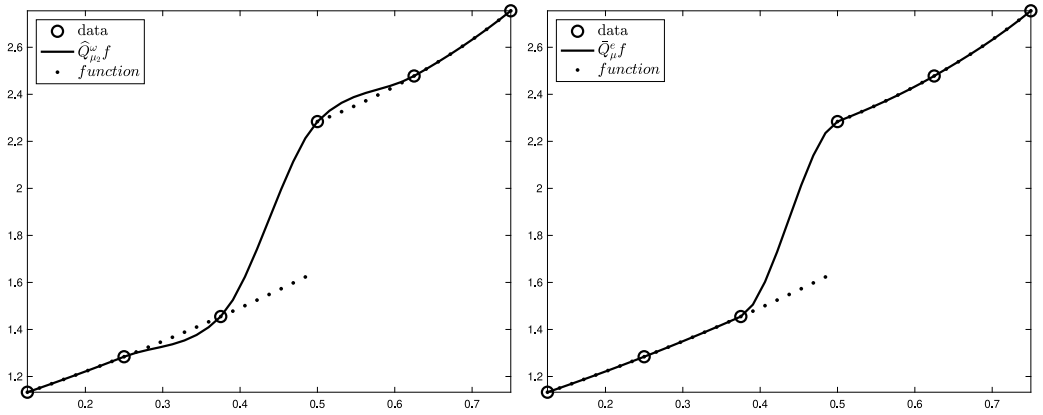

Fig. 6. Reconstructions of a discontinuous function (19) with $\widehat{Q}^{\omega}_{\mu_2} f$ (left) and $\bar{Q}^{e}_{\mu} f$ (right).

then, if f is smooth, it holds

- $\bar{Q}^{e}_{\mu} f$ *is* C^1*-continuous,*
- $\bar{Q}^{e}_{\mu} f = f$ *for all* $f \in \mathbb{P}_3$,
- $\left\| \overline{Q}^{e}_{\mu} f - f \right\|_{\infty, I} = \mathcal{O}(h^4)$ *for all* $f \in C^4(I)$,

and if f has a discontinuity at (x_{i-1}, x_i) then

- $\bar{Q}^{e}_{\mu} f$ *is* C^1*-continuous,*
- $\left\| \overline{Q}^{e}_{\mu} f - f \right\|_{\infty, [a, x_{i-1}] \cup [x_i, b]} = \mathcal{O}(h^4)$.

Proof. The claims in both cases are stated from the fact that $\overline{Q}^{p}_{\mu} f = f$, $f \in \mathbb{P}_3$, $p = \ell, r$. □

In Fig. 6 we see the results that we obtain with the techniques of this and the previous sections. It is clear that WENO with four points cannot eliminate the oscillations around the singularity, as shown in Fig. 6 (left) on the left. However, the ENO technique with four points yields good results (Fig. 6, right).

6. Numerical experiments

In this section we show numerical experiments that corroborate the theoretical results presented in this paper.

6.1. Order of reconstruction

We consider the interval $I = [0, 1]$ and the discontinuous function

$$f(x) := \begin{cases} e^x, & \text{if } 0 \le x < 0.5, \\ 1 + e^{x^2}, & \text{if } 0.5 \le x \le 1. \end{cases} \tag{19}$$

We use the set of grids P_{N_k} with $N_k = 2^k$, $k = 6, \ldots, 11$, to obtain different approximations $\hat{f}^k(x) := Qf(x)$ to $f(x)$. We calculate the approximation errors on the intervals $[c, 1]$, $c \in \{x^k_{N_k/2}, x^k_{N_k/2+1}, x^k_{3N_k/4}\}$, by

$$e^c_k := \sup_{x \in [c,1]} \{ |\hat{f}^k(x) - f(x)| \}.$$

For $c = x^k_{3N_k/4} = 0.75$, we are evaluating the error on a smooth area. For $c = x^k_{N_k/2} = 0.5$ we have a region next to a discontinuity. The value $c = x^k_{N_k/2+1}$ is used due to theoretical results in Theorem 13. We also evaluate $\log_2(e^c_{k+1}/e^c_k)$ for $k = 4, \ldots, 8$. Note that if $e^c_k = O(\frac{1}{N^n_k})$ then $\log_2(e^c_{k+1}/e^c_k) \approx n$. We use all the methods presented in this paper, which are Q_{μ_1} (Theorem 4), Q_{μ_2} (Theorem 4), $Q^{\omega}_{\mu_2}$ (Theorem 6), $Q^{\omega}_{\mu_1}$ (Theorem 9), $\widehat{Q}^{\omega}_{\mu_2}$ (Theorem 13) and $\bar{Q}^{e}_{\mu}$ (Theorem 18) (see Tables 1–3).

6.2. Reconstruction

Now, we give some graphical results to confirm the reduction of the Gibbs phenomenon using the WENO technique. Now, we discretize function (19) with $2^3 + 1 = 9$ points and from them we reconstruct the function with different QI operators. In Figs. 7–9 we see the results we obtain. In Figs. 4–6 we see a zoom of these figures.

Table 1
Numerical orders of approximation $\log_2(e^c_{k+1}/e^c_k)$ for different QI splines and $c = x^k_{3N_k/4} = 0.75$ (smooth area [[0.75, 1]).

Q_{μ_1}	Q_{μ_2}	$Q^{\omega}_{\mu_2}$	$Q^{\omega}_{\mu_1}$	$\hat{Q}^{\omega}_{\mu_2}$	$\bar{Q}^{e}_{\mu}$
3.98	3.97	4.02	3.98	3.97	3.91
3.99	3.99	3.99	3.98	3.99	3.94
3.99	3.99	3.99	3.99	3.99	3.97
4.00	4.00	4.00	4.00	4.00	3.99
4.00	3.99	3.97	4.00	3.99	3.99

Table 2
Numerical orders of approximation $\log_2(e^c_{k+1}/e^c_k)$ for different QI splines and $c = x^k_{2N_k/2} = 0.5$ (next to a discontinuity [0.5, 1]).

Q_{μ_1}	Q_{μ_2}	$Q^{\omega}_{\mu_2}$	$Q^{\omega}_{\mu_1}$	$\hat{Q}^{\omega}_{\mu_2}$	$\bar{Q}^{e}_{\mu}$
0.00	0.01	3.03	2.03	0.01	3.91
0.00	0.00	3.01	2.01	0.00	3.94
0.00	0.00	3.01	2.01	0.00	3.97
0.00	0.00	3.00	2.00	0.00	3.99
0.00	0.00	3.00	2.00	0.00	3.99

Table 3
Numerical orders of approximation $\log_2(e^c c_{k+1}/e^c_k)$ for different QI splines and $c = x^k_{2N_k/2+1}$ (close to a discontinuity $[x^k_{N_k/2+1}, 1]$.

Q_{μ_1}	Q_{μ_2}	$Q^{\omega}_{\mu_2}$	$Q^{\omega}_{\mu_1}$	$\hat{Q}^{\omega}_{\mu_2}$	$\bar{Q}^{e}_{\mu}$
0.01	0.01	3.03	2.03	3.97	3.91
0.00	0.00	3.01	2.02	3.99	3.94
0.00	0.00	3.01	2.01	3.99	3.97
0.00	0.00	3.00	2.00	4.00	3.99
0.00	0.00	3.00	2.00	3.99	3.99

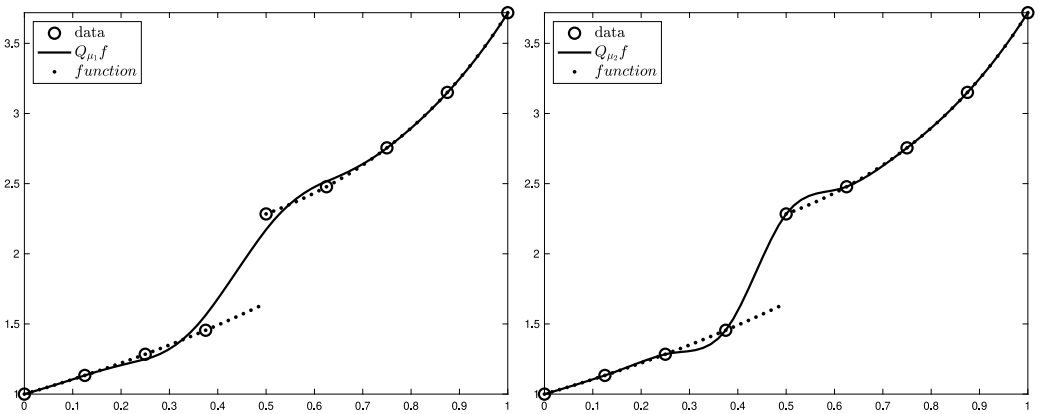

Fig. 7. Reconstruction with Q_{μ_1} (left) and Q_{μ_2} (right).

Finally, we consider $u_0(x)$ taken from [20] and which a function that is the initial condition of a conservation laws equation.

$$u_0(x) = \begin{cases} (G(x, z-\delta) + G(x, z+\delta) + 4\,G(x, z))/6, & -0.8 \le x \le -0.6, \\ 1, & -0.4 \le x \le -0.2, \\ 1 - |10\,(x - 0.1)|, & 0 \le x \le 0.2, \\ (F(x, a-\delta) + F(x, a+\delta) + 4\,F(x, a))/6, & 0.4 \le x \le 0.6, \\ 0, & \text{otherwise}, \end{cases} \tag{20}$$

where $G(x, z) = e^{-\beta(x-z)^2}$ and $F(x, a) = \max(1 - \alpha^2(x-a), 0)^{1/2}$. We take the constants $a = 0.5$, $z = -0.7$, $\delta = 0.005$, $\alpha = 10$ and $\beta = \frac{log2}{36\delta^2}$.

The function (20) is discretized with $N_5 = 2^5$ values and with them we have applied the Q_{μ_2} and $Q^{w}_{\mu_2}$ methods. In Fig. 10 we show the obtained results. It is clear that the reconstruction obtained from $Q^{w}_{\mu_2}$ is better than Q_{μ_2}. We observe that the use of linear

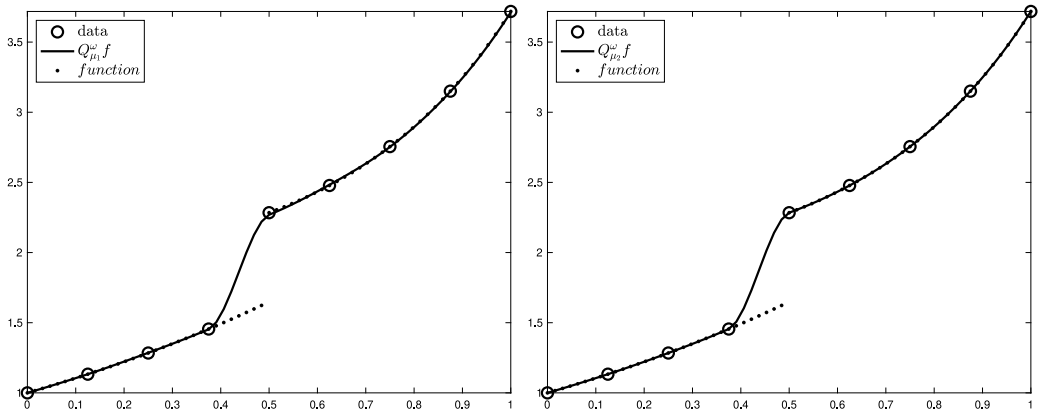

Fig. 8. Reconstructions with $Q^{\omega}_{\mu_1}$ (left) and $Q^{\omega}_{\mu_2}$ (right).

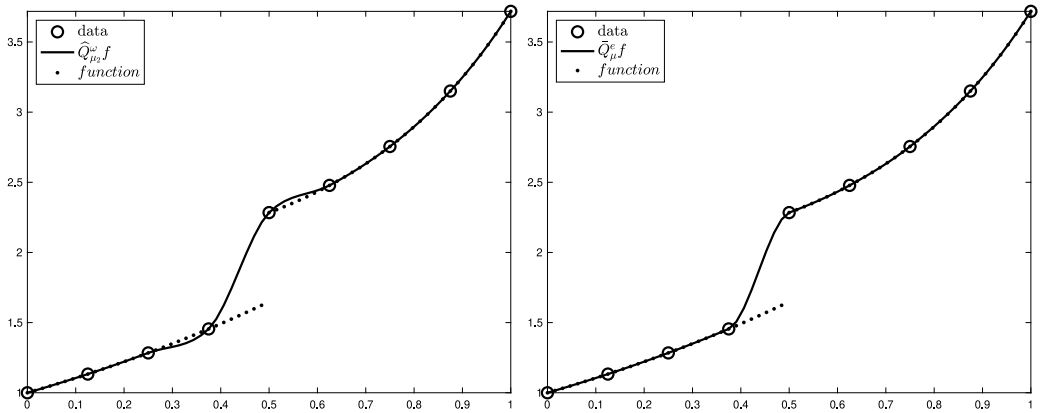

Fig. 9. Reconstructions with Left $\hat{Q}^{\omega}_{\mu_2}$ (left) and $\bar{Q}^{e}_{\mu}$ (right).

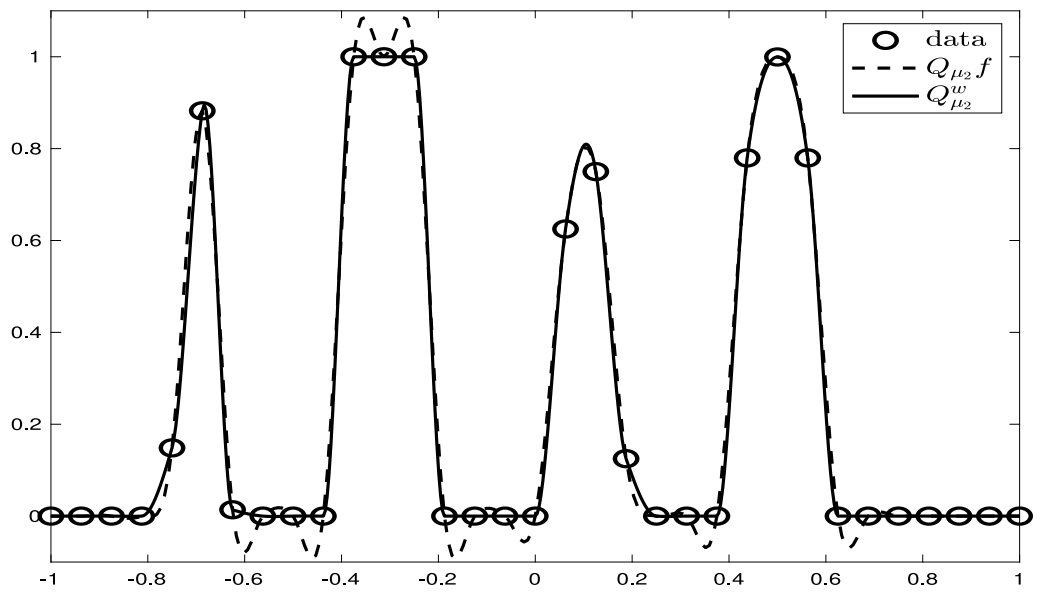

Fig. 10. Reconstructions with different cubic QI splines. $\hat{Q}^{\omega}_{\mu_2}$, right $\bar{Q}^{e}_{\mu}$.

spline schemes causes oscillations around the jumps, whereas non-linear enhancement based on the WENO technique ensures the avoidance of these oscillations.

7. Conclusion

In this paper several non-linear spline schemes in Bernstein–Bézier form are presented. All of them are optimal in smooth regions, and have different behaviors and orders of accuracy near the singularity point.

The construction used here allows a direct choice of positive weights for the WENO technique, which permits us to avoid supplementary treatment whenever negative weights appear.

CRediT authorship contribution statement

F. Aràndiga: Conceptualization, Data curation, Formal analysis, Funding acquisition, Investigation, Methodology, Project administration, Resources, Software, Supervision, Validation, Visualization, Writing – original draft, Writing – review & editing. **D. Barrera:** Conceptualization, Data curation, Formal analysis, Funding acquisition, Investigation, Methodology, Project administration, Resources, Software, Supervision, Validation, Visualization, Writing – original draft, Writing – review & editing. **S. Eddargani:** Conceptualization, Data curation, Formal analysis, Funding acquisition, Investigation, Methodology, Project administration, Resources, Software, Supervision, Validation, Visualization, Writing – original draft, Writing – review & editing.

Acknowledgments

The authors wish to thank the anonymous referees for their very pertinent and useful comments which helped them to improve the original manuscript. The first author acknowledges the funding provided by the Spanish MINECO project PID2020-117211GB-I00 and GVA project CIAICO/2021/227. The second author is a member of the research group FQM 191 Matemática Aplicada funded by the PAIDI programme of the Junta de Andalucía, Spain. The third author is a member of the research group GNCS of Italy and acknowledges the support of the MUR Excellence Department Project awarded to the Department of Mathematics, University of Rome Tor Vergata, CUP E83C23000330006.

References

[1] A. Abbadi, D. Barrera, M.J. Ibáñez, D. Sbibih, A general method for constructing quasi-interpolants from B-splines, J. Comput. Appl. Math. 234 (4) (2010) 1324–1337.
[2] F. Aràndiga, A. Baeza, A.M. Belda, P. Mulet, Analysis of WENO schemes for full and global accuracy, SIAM J. Numer. Anal. 49 (2) (2011) 893–915.
[3] F. Aràndiga, A.M. Belda, Weighted ENO interpolation and applications, Commun. Nonlinear Sci. Numer. Simul. 9 (2004) 187–195.
[4] F. Aràndiga, R. Donat, S.L. Ureña, Nonlinear improvements of quasi-interpolanting splines to approximate piecewise smooth functions, Appl. Math. Comput. 448 (1) (2023) 127946.
[5] D. Barrera, C. Dagnino, M.J. Ibáñez, S. Remogna, Point and differential quasi-interpolation on three direction meshes, J. Comput. Appl. Math. 354 (2019) 373–389.
[6] D. Barrera, S. Eddargani, M.J. Ibáñez, S. Remogna, Low-degree spline quasi-interpolants in the Bernstein basis, Appl. Math. Comput. 457 (2023) 128150.
[7] D. Barrera, S. Eddargani, M.J. Ibáñez, S. Remogna, Spline quasi-interpolation in the Bernstein basis on the Powell–Sabin 6-split of a type-1 triangulation, J. Comput. Appl. Math. 424 (2023) 115011.
[8] D. Barrera, S. Eddargani, A. Lamnii, A novel construction of B-spline-like bases for a family of many knot spline spaces and their application to quasi-interpolation, J. Comput. Appl. Math. 404 (2022) 113761.
[9] J.M. Carnicer, J.M. Peña, Totally positive bases for shape preserving curve design and optimality of B-splines, Comput. Aided Geom. Design 11 (1994) 633–654.
[10] C.K. Chui, H. Diamond, A natural formulation of quasi-interpolation by multivariate splines, Proc. Am. Math. 99 (4) (1987) 643–646.
[11] C. Dagnino, P. Lamberti, S. Remogna, On spline quasi-interpolation through dimensions, Annali Dell'Univ. Di Ferrara 68 (2022) 397–415.
[12] J.M. Davis, P. Hagelstein, Gibbs phenomena for some classical orthogonal polynomials, J. Math. Anal. Appl. 505 (2022) 125574.
[13] C. de Boor, Splines as linear combinations of B-spline, Approximation Theory II, Academic Press, New York, 1976, pp. 1–47,
[14] R.A. DeVore, G.G. Lorenta, Constructive Approximation, Springer Berlin, Heidelberg, 1993.
[15] S. Eddargani, A. Lamnii, M. Lamnii, On algebraic trigonometric integro splines, Z. Angew. Math. Mech. 100 (2020) e201900262.
[16] S. Eddargani, A. Lamnii, M. Lamnii, D. Sbibih, A. Zidna, Algebraic hyperbolic spline quasi-interpolants and applications, J. Comput. Appl. Math. 347 (2019) 196–209.
[17] P. Fan, Y. Shen, B. Tian, C. Yang, A new smoothness indicator for improving the weighted essentially non-oscillatory scheme, J. Comput. Phys. 269 (2014) 329–354.
[18] A. Harten, B. Engquist, S. Osher, S. Chakravarthy, Uniformly high order essentially non-oscillatory schemes III, J. Comput. Phys. 71 (1987).
[19] G.S. Jiang, C.W. Shu, Efficient implementation of weighted ENO schemes, J. Comput. Phys. 126 (1) (1996) 202–228.
[20] D. Levy, G. Puppo, G. Russo, Central WENO schemes for hyperbolic systems of conservation laws, ESAIM Math. Model. Numer. Anal. 33 (3) (1999) 547–571.
[21] X.D. Liu, S. Osher, T. Chan, Weighted essentially non-oscillatory schemes, J. Comput. Phys. 115 (1) (1994) 200–212.
[22] P. Sablonnière, D. Sbibih, Integral spline operators exact on polynomials, Approx. Theory Appl. 10 (1994) 56–73.
[23] P. Sablonnière, D. Sbibih, M. Tahrichi, High-order quadrature rules based on spline quasi-interpolants and application to integral equations, Appl. Numer. Math. 62 (2012) 507–520.
[24] I.J. Schoenberg, Contributions to the problem of approximation of equidistant data by analytic functions. Part A. On the problem of smoothing or graduation. A first class of analytic approximation formulae, Quart. Appl. Math. 4 (1946) 45–99.
[25] I.J. Schoenberg, Contributions to the problem of approximation of equidistant data by analytic functions. Part B. On the problem of osculatory interpolation, a second class of analytic approximation formulae, Quart. Appl. Math. 4 (1946) 112–141.
[26] J. Shi, C. Hu, C. Shu, A technique of treating negative weights in WENO schemes, J. Comput. Phys. 175 (2002) 108–127.
[27] T. Sorokina, F. Zeilfelder, An explicit quasi-interpolation scheme based on C^1 quartic splines on type-1 triangulations, Comput. Aided Geom. Design 25 (2008) 1–13.